

## Drug Discovery: Recent Progress and the Future

## Regular Article

## Different Degradation Mechanisms of Inhibitor of Apoptosis Proteins (IAPs) by the Specific and Nongenetic IAP-Dependent Protein Eraser (SNIPER)

Nobumichi Ohoka,<sup>\*,a</sup> Osamu Ujikawa,<sup>b,†</sup> Kenichiro Shimokawa,<sup>b</sup> Tomoya Sameshima,<sup>b</sup> Norihito Shibata,<sup>a</sup> Takayuki Hattori,<sup>a</sup> Hiroshi Nara,<sup>b,‡</sup> Nobuo Cho,<sup>b,§</sup> and Mikihiro Naito<sup>\*,a</sup>

<sup>a</sup>Division of Molecular Target and Gene Therapy Products, National Institute of Health Sciences; 3–25–26 Tonomachi, Kawasaki 210–9501, Japan; and <sup>b</sup>Pharmaceutical Research Division, Takeda Pharmaceutical Co., Ltd.; 2–26–1 Muraoka-Higashi, Fujisawa, Kanagawa 251–8555, Japan.

Received July 25, 2018; accepted September 21, 2018;

advance publication released online October 26, 2018

Targeted protein degradation by small molecules is an emerging modality with significant potential for drug discovery. We previously developed chimeric molecules, termed specific and non-genetic inhibitor of apoptosis protein (IAP)-dependent protein erasers (SNIPERs), which induce the ubiquitylation and proteasomal degradation of target proteins. This degradation is mediated by the IAPs; the target proteins include bromodomain-containing protein 4 (BRD4), an epigenetic regulator protein. The SNIPER that degrades this particular protein, SNIPER(BRD)-1, consists of an IAP antagonist LCL-161 derivative and a bromodomain and extra-terminal (BET) inhibitor, (+)-JQ-1. SNIPER(BRD)-1 also degrades a cellular inhibitor of apoptosis protein 1 (cIAP1) and an X-linked inhibitor of apoptosis protein (XIAP), the mechanisms of which are not well understood. Here, we show that the degradation of cIAP1 and XIAP by SNIPER(BRD)-1 is induced *via* different mechanisms. Using a chemical biology-based approach, we developed two inactive SNIPERs, SNIPER(BRD)-3 and SNIPER(BRD)-4, incapable of degrading BRD4. SNIPER(BRD)-3 contained an *N*-methylated LCL-161 derivative as the IAP ligand, which prevented it from binding IAPs, and resulted in the abrogated degradation of cIAP1, XIAP, and BRD4. SNIPER(BRD)-4, however, incorporated the enantiomer (–)-JQ-1 which was incapable of binding BRD4; this SNIPER degraded cIAP1 but lost the ability to degrade XIAP and BRD4. Furthermore, a mixture of the ligands, (+)-JQ-1 and LCL-161, induced the degradation of cIAP1, but not XIAP and BRD4. These results indicate that cIAP1 degradation is triggered by the binding of the IAP antagonist module to induce autoubiquitylation of cIAP1, whereas a ternary complex formation is required for the SNIPER-induced degradation of XIAP and BRD4.

**Key words** ubiquitin; proteasome; E3 ligase; chimeric small molecule

## Introduction

Targeted protein degradation with small molecules is an emerging technology that has significant potential for drug discovery. We and other groups have developed protein knockdown systems using chimeric small molecules to induce the selective degradation of target proteins in cells.<sup>1–4)</sup> The two classes of these chimeric molecules, termed specific and non-genetic inhibitor of apoptosis protein (IAP)-dependent protein erasers (SNIPERs), and proteolysis targeting chimeras (PROTACs), are composed of two different ligands connected by a linker: one ligand is specific for the target protein and the other is specific for an E3 ubiquitin ligase, which cross-

links these proteins to induce selective ubiquitylation and proteasomal degradation of the target protein. For the PROTACs, recruitment of the von Hippel–Lindau (VHL) and cereblon (CRBN) E3 ligase complex is enabled by the incorporation of a VHL ligand and a thalidomide derivative into the PROTAC constructs as the E3 ligand. For the SNIPERs, an IAP antagonist is integrated into the SNIPER constructs to recruit the cellular inhibitor of apoptosis protein 1 (cIAP1) and an X-linked inhibitor of apoptosis protein (XIAP) E3 ligases. To date, a range of PROTAC and SNIPER compounds have been developed, allowing the degradation of a variety of proteins such as estrogen receptor  $\alpha$  (ER $\alpha$ ), BCR-ABL, and bromodomain-containing protein 4 (BRD4).<sup>5–15)</sup> Some PROTACs and SNIPERs have demonstrated the ability to degrade target proteins and suppress tumor growth *in vivo*, suggesting that this technology is feasible for novel drug discovery. These include VHL-based and CRBN-based PROTACs designed against BRD4, which are capable of degrading BRD4 protein in mouse xenograft models.<sup>16–18)</sup> By incorporating LCL-161 derivatives as a high-affinity IAP ligand, we previously de-

<sup>†</sup>Present address: Axcelead Drug Discovery Partners, Inc.; 2–26–1 Muraoka-Higashi, Fujisawa, Kanagawa 251–0012, Japan.

<sup>‡</sup>Present address: The Pharmaceutical Society of Japan; 2–12–15 Shibuya, Shibuya-ku, Tokyo 150–0002, Japan.

<sup>§</sup>Present address: Drug Discovery Chemistry Platform Unit, Drug Discovery Platforms Cooperation Division, RIKEN Center for Sustainable Resource Science; 2–1 Hirosawa, Wako, Saitama 351–0198, Japan.

\* To whom correspondence should be addressed. e-mail: n-ohoka@nihs.go.jp; miki-naito@nihs.go.jp

veloped SNIPER(ER)-87 and -110 that induce the *in vivo* degradation of ER $\alpha$  and growth inhibition of an ER $\alpha$ -positive human breast tumor in a xenograft model.<sup>11,19</sup>

IAPs are a family of anti-apoptotic proteins that contain one or three baculovirus IAP repeat (BIR) domains.<sup>20–22</sup> Some family members, such as cIAP1, cIAP2, and XIAP, bind to and regulate caspases *via* the BIR domains, thereby inhibiting apoptosis.<sup>23–26</sup> These IAPs are attractive therapeutic targets against cancer because IAPs are involved in resistance to cancer therapy and poor prognosis.<sup>27–33</sup> To date, several IAP antagonists have been developed; some of these are under evaluation in clinical trials as anticancer drugs.<sup>20,34,35</sup> IAP antagonists interact with the BIR domains in IAP proteins to directly suppress the inhibitory activity of XIAP towards caspases or to induce the autoubiquitylation and proteasomal degradation of cIAP1 and cIAP2.<sup>36–39</sup> Because SNIPERs contain high-affinity IAP antagonists as IAP ligand modules, SNIPERs downregulate cIAP1 and XIAP along with their intrinsic target proteins, which is likely to be advantageous when attempting to kill cancer cells that require IAPs for survival.<sup>6,11,19</sup> However, the degradation mechanisms of IAPs by the SNIPERs is not well understood. In this study, we analyzed the degradation mechanisms of cIAP1 and XIAP induced by SNIPER(BRD)s that specifically degrade BRD proteins.

## Results and Discussion

We previously developed SNIPER(BRD)-1 by conjugating an LCL-161 derivative to (+)-JQ-1, a bromodomain and extraterminal (BET) inhibitor (Fig. 1), which induces the degradation of BRD4 *via* the ubiquitin–proteasome pathway in LNCaP

human prostate tumor cells.<sup>11</sup> SNIPER(BRD)-2 (**11a**) has a longer linker than SNIPER(BRD)-1 (Fig. 1). Both SNIPERs were observed to rapidly reduce BRD4 protein levels within 6h of treatment, with an optimal concentration of 0.1  $\mu$ M (Fig. 2A). In addition to BRD4, SNIPER(BRD)-1 effectively reduced the protein levels of cIAP1 and XIAP within 6h (Fig. 2B).

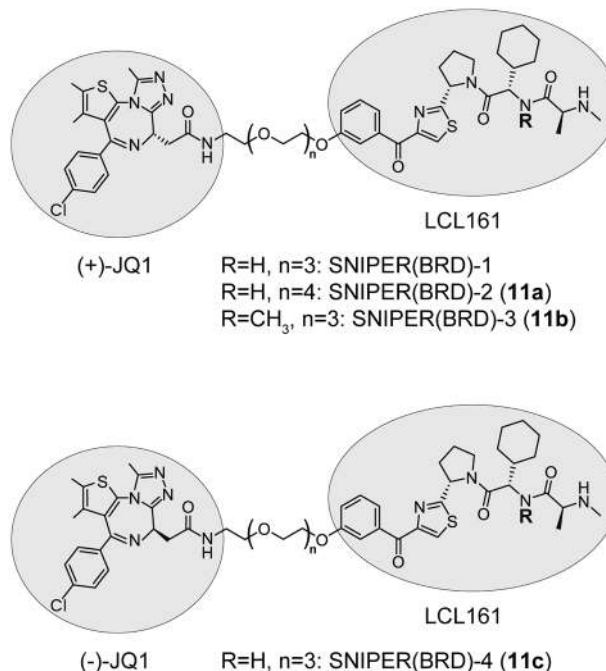


Fig. 1. Chemical Structures of the Four SNIPER(BRD)s

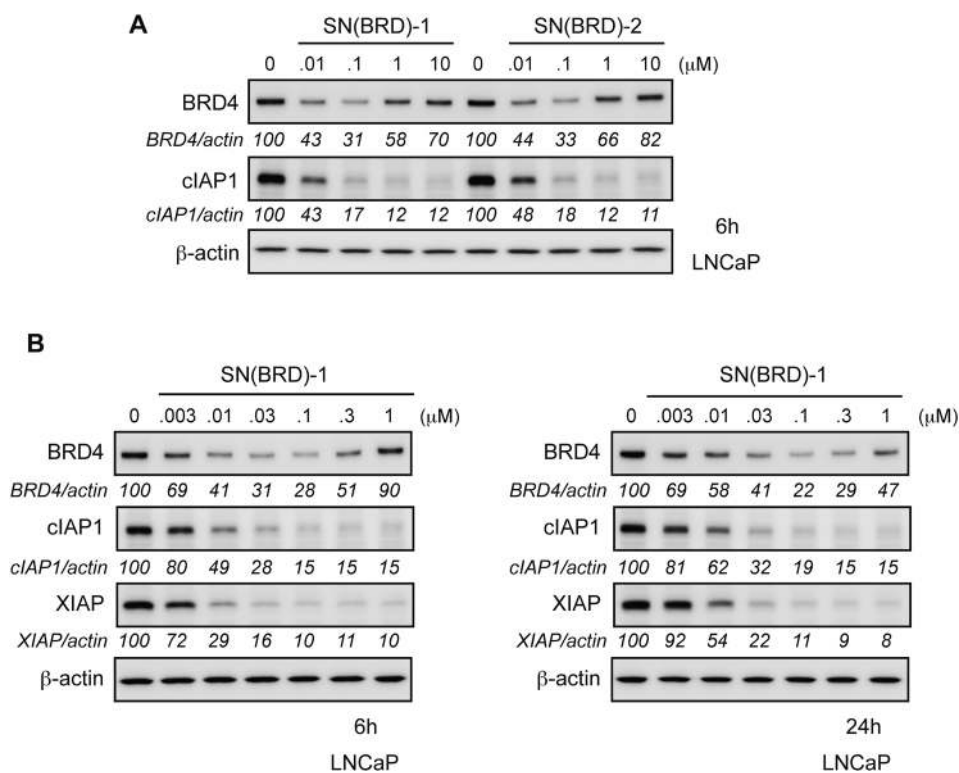


Fig. 2. SNIPER(BRD) Degradation of cIAP1, XIAP, and BRD4

(A, B) LNCaP cells were treated with increasing concentrations of SNIPER(BRD)-1 or SNIPER(BRD)-2 for the indicated time periods. Whole-cell lysates were analyzed by Western blotting with specific antibodies. Numbers below the BRD4, cIAP1, and XIAP panels represent the BRD4/actin, cIAP1/actin, and XIAP/actin ratios, respectively, normalized by designating the expression from the vehicle control condition as 100%. SN(BRD): SNIPER(BRD).

SNIPER(BRD)-3 (**11b**), in which an *N*-methylated analog of the LCL-161 derivative was conjugated, was incapable of binding IAP proteins (Fig. 1 and Table 1). Consequently, SNIPER(BRD)-3 did not induce the degradation of BRD4, cIAP1 or XIAP (Fig. 3). This result indicates that IAP-binding ability is critical for the degradation of BRD4 and IAP proteins by SNIPER(BRD)-1. The addition of a free IAP ligand, LCL-161, either alone or in combination with the BRD4 ligand, (+)-JQ-1, decreased the level of cIAP1 but not BRD4 and XIAP (Fig. 4A), suggesting that the degradation of BRD4 and XIAP requires a ternary complex formation composed of BRD4, SNIPER, and XIAP.

To further investigate whether BRD4-binding ability is required for XIAP degradation by SNIPER(BRD)-1, the (+)-JQ-1 moiety of SNIPER(BRD)-1 was substituted with the enantiomer (–)-JQ-1 that cannot bind to BRD4 (Fig. 1). The

resulting SNIPER(BRD)-4 (**11c**) did not degrade BRD4 or XIAP (Fig. 4B). This finding confirms that cross-linking to the target protein is critical for the SNIPER(BRD)-1-mediated degradation of XIAP. SNIPER(BRD)-4 did, however, induce the degradation of cIAP1, indicating that BRD4-binding ability is not required for the SNIPER(BRD)-1-mediated degradation of cIAP1, which is consistent with the degradation of

Table 1. IAP-Binding Affinities of the SNIPER(BRD)s

Compound	IC <sub>50</sub> (95% CI) (nM)		
	cIAP1	cIAP2	XIAP
SNIPER(BRD)-1	6.8 (5.6–8.1)	17 (13–22)	49 (39–62)
SNIPER(BRD)-2	13 (12–14)	22 (20–24)	77 (70–84)
SNIPER(BRD)-3	>1000	>1000	>1000
SNIPER(BRD)-4	10 (9.7–11)	8.4 (7.5–9.4)	47 (37–59)

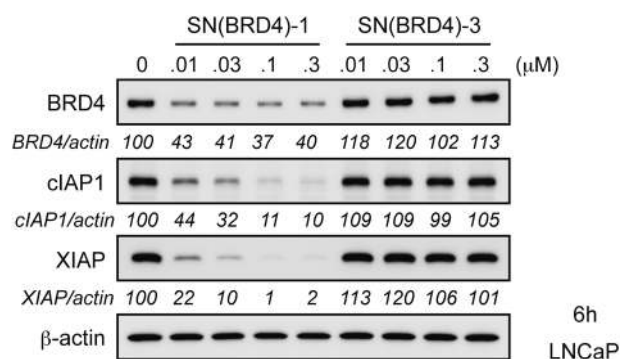


Fig. 3. SNIPER(BRD) with an Inactive IAP Ligand Loses Its Protein-Knockdown Activity

LNCaP cells were treated with increasing concentrations of SNIPER(BRD)-1 or SNIPER(BRD)-3 for 6 h. Whole-cell lysates were analyzed by Western blotting with specific antibodies. Numbers below the BRD4, cIAP1, and XIAP panels represent the BRD4/actin, cIAP1/actin, and XIAP/actin ratios, respectively, normalized by designating the expression from the vehicle control condition as 100%.

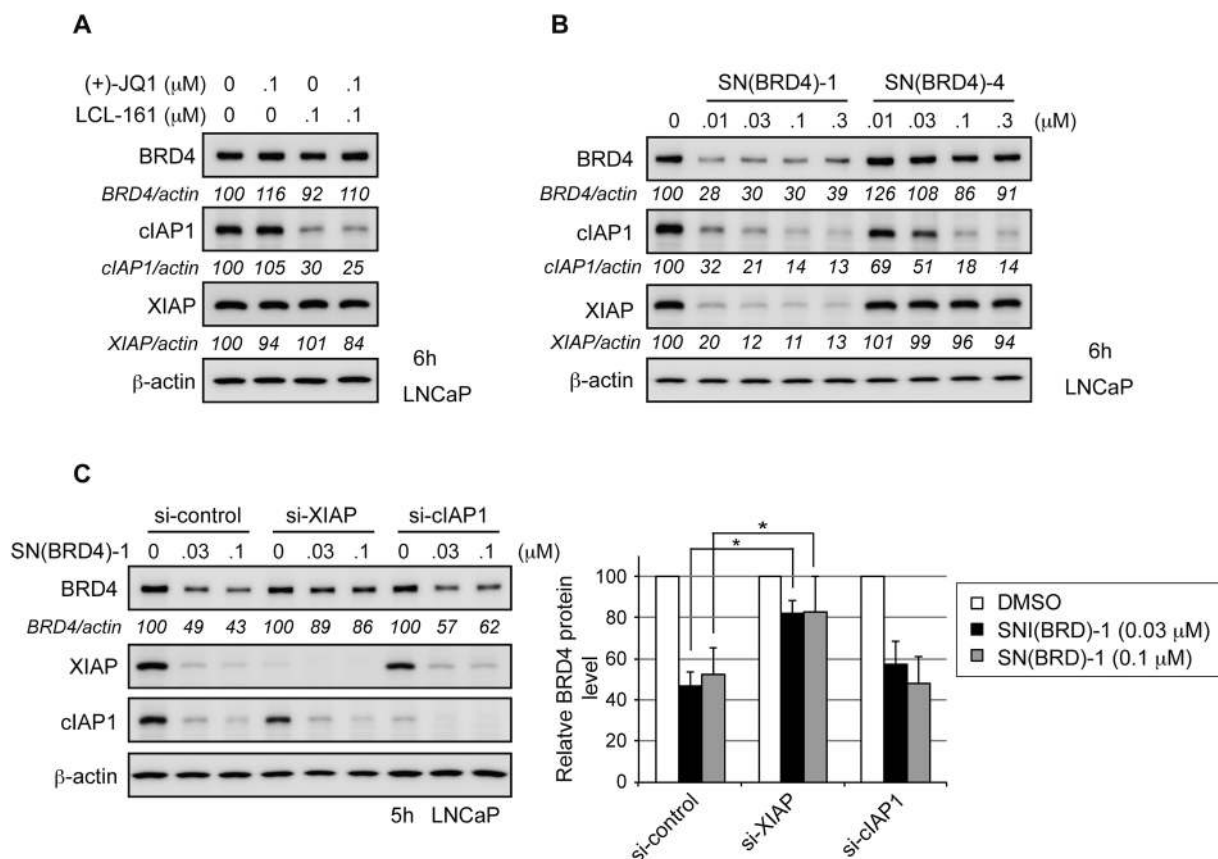


Fig. 4. Degradation of BRD4 and XIAP Requires the Formation of a Ternary SNIPER Complex

(A) LNCaP cells were treated with the indicated concentrations of (+)-JQ1 and LCL-161 for 6 h. (B) LNCaP cells were treated with increasing concentrations of either SNIPER(BRD)-1 or SNIPER(BRD)-4 for 6 h. (C) SNIPER(BRD)-1 preferentially utilizes XIAP to degrade BRD4. LNCaP cells were transfected with the indicated siRNA for 42 h and treated with SNIPER(BRD)-1 for 5 h. Whole-cell lysates were analyzed by Western blotting with specific antibodies. Numbers below the BRD4, cIAP1, and XIAP panels represent the BRD4/actin, cIAP1/actin, and XIAP/actin ratios, respectively, normalized by designating the expression from the vehicle control condition as 100%. Data in the bar graph are the mean ± standard deviation (S.D.) (error bars) of four independent experiments; asterisks indicate  $p < 0.01$  compared with control siRNA.



cIAP1 by a free IAP ligand, LCL-161 (Fig. 4A).

Thus, SNIPER(BRD)-1 degrades cIAP1 and XIAP along with the intrinsic target BRD4; however, the degradation mechanism clearly differs for each IAP protein. The degradation of cIAP1 by SNIPER(BRD)-1 requires IAP-binding ability (Fig. 3) but not BRD4-binding ability (Fig. 4B), suggesting that binding of the IAP antagonist module of SNIPER(BRD)-1 to the BIR domain of cIAP1 induces its autoubiquitylation and proteasomal degradation. This is consistent with previous observations that many IAP antagonists, including LCL-161, induce autoubiquitylation and proteasomal degradation of cIAP1 but not XIAP. In contrast, XIAP degradation requires ternary complex formation comprising BRD4, SNIPER, and XIAP, because treatment using a mixture of the ligands (Fig. 4A), a structural analog of SNIPER(BRD) that cannot bind to IAPs (Fig. 3), and an analog that cannot bind to BRD4 (Fig. 4B) do not result in the degradation of XIAP. Consistent with these results, we previously observed that XIAP degradation by LCL-161-based SNIPERs directed against ER $\alpha$  was not

observed in cells that did not express ER $\alpha$ , while XIAP degradation was prominently observed in cells that expressed more ER $\alpha$  than XIAP.<sup>19</sup> Taken together, these results convincingly indicate that XIAP in the ternary complex is subjected to degradation together with the intrinsic target protein by SNIPERs.

We previously reported that LCL-161-based SNIPERs directed against ER $\alpha$  preferentially utilize XIAP to degrade ER $\alpha$  along with the XIAP itself. To investigate whether XIAP is the primary E3 ligase responsible for the BRD4 degradation by SNIPER(BRD)-1, we examined the effect of cIAP1 and XIAP depletion by small interfering RNA (siRNA). Depletion of XIAP substantially suppressed the BRD4 degradation induced by SNIPER(BRD)-1, whereas depletion of cIAP1 hardly suppressed the degradation (Fig. 4C). This result suggests that SNIPER(BRD)-1 preferentially recruits XIAP to degrade BRD4, which results in the efficient degradation of XIAP.

We further observed that the SNIPER(BRD)-1-induced degradation of XIAP protein was abrogated by the proteasome inhibitor, MG132, and the ubiquitin-activating enzyme inhibitor, MLN7243 (Fig. 5), indicating that SNIPER(BRD)-1 induces degradation of XIAP *via* the ubiquitin–proteasome pathway. Notably, the ladder of slower migrating protein bands for XIAP was clearly detected when cells had been treated with SNIPER(BRD)-1 in the presence of MG132 (Fig. 5), confirming that the XIAP protein was ubiquitylated upon treatment with SNIPER(BRD)-1.

The protein degradation efficacy by SNIPER and PROTAC molecules was often suppressed at higher concentrations, which is known as a hook effect. This effect is explained by the inhibition of a ternary complex formation by an excess amount of SNIPERs and PROTACs when a single type of target is cross-linked to single E3s (Fig. S1). However, given that both BRD4 and XIAP in the ternary complex are degraded, it is puzzling that the pharmacological hook effect was only observed for the degradation of BRD4 but not of XIAP (*i.e.*, decreasing levels of BRD4 degradation were observed with increasing SNIPER concentrations; Fig. 2). Because (+)-JQ-1 interacts with other BRD proteins such as BRD2 and BRD3,<sup>40</sup>

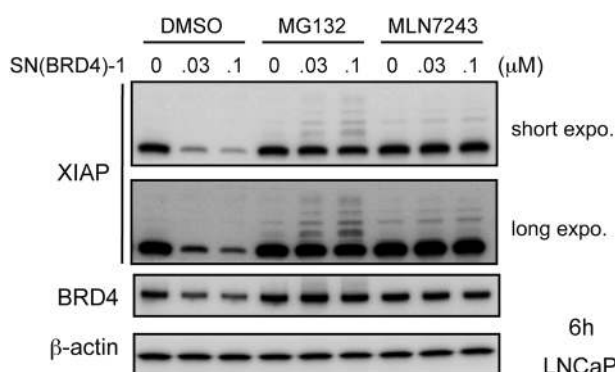


Fig. 5. SNIPER(BRD)-1 Degrades XIAP and BRD4 *via* the Ubiquitin–Proteasome Pathway

LNCaP cells were treated for 6h with increasing concentrations of SNIPER(BRD4)-1 in the presence of 10  $\mu$ M of either dimethyl sulfoxide (DMSO), MG132 or MLN7243. Whole-cell lysates were analyzed by Western blotting with specific antibodies. Actin was used as the loading control.

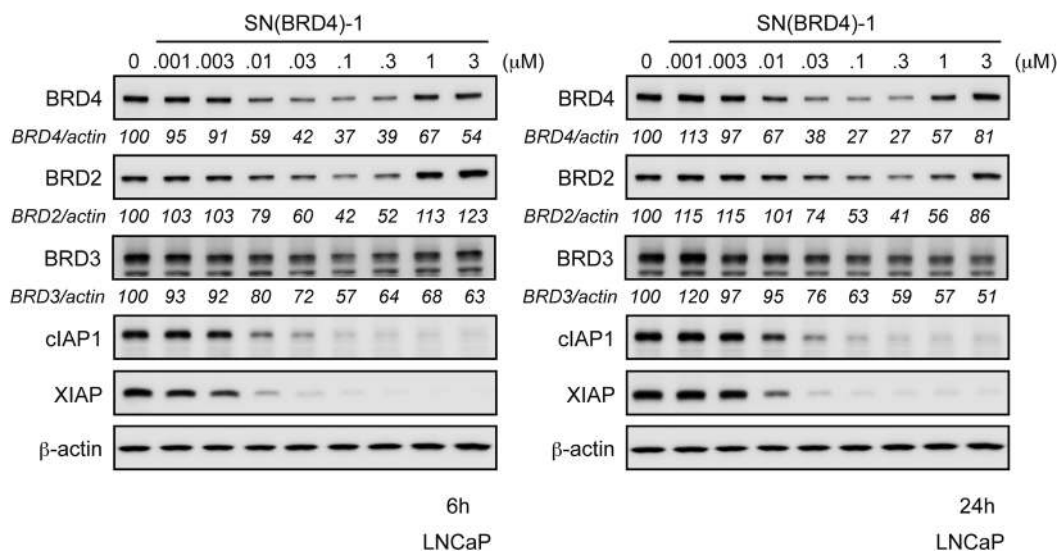


Fig. 6. SNIPER(BRD)-1 also Induces the Degradation of BRD2 and BRD3

LNCaP cells were treated with increasing concentrations of SNIPER(BRD)-1 for 6 or 24h. Whole-cell lysates were analyzed by Western blotting with specific antibodies. Numbers below the BRD4, BRD2, and BRD3 panels represent the BRD4/actin, BRD2/actin, and BRD3/actin ratios, respectively, normalized by designating the expression from the vehicle control condition as 100%.

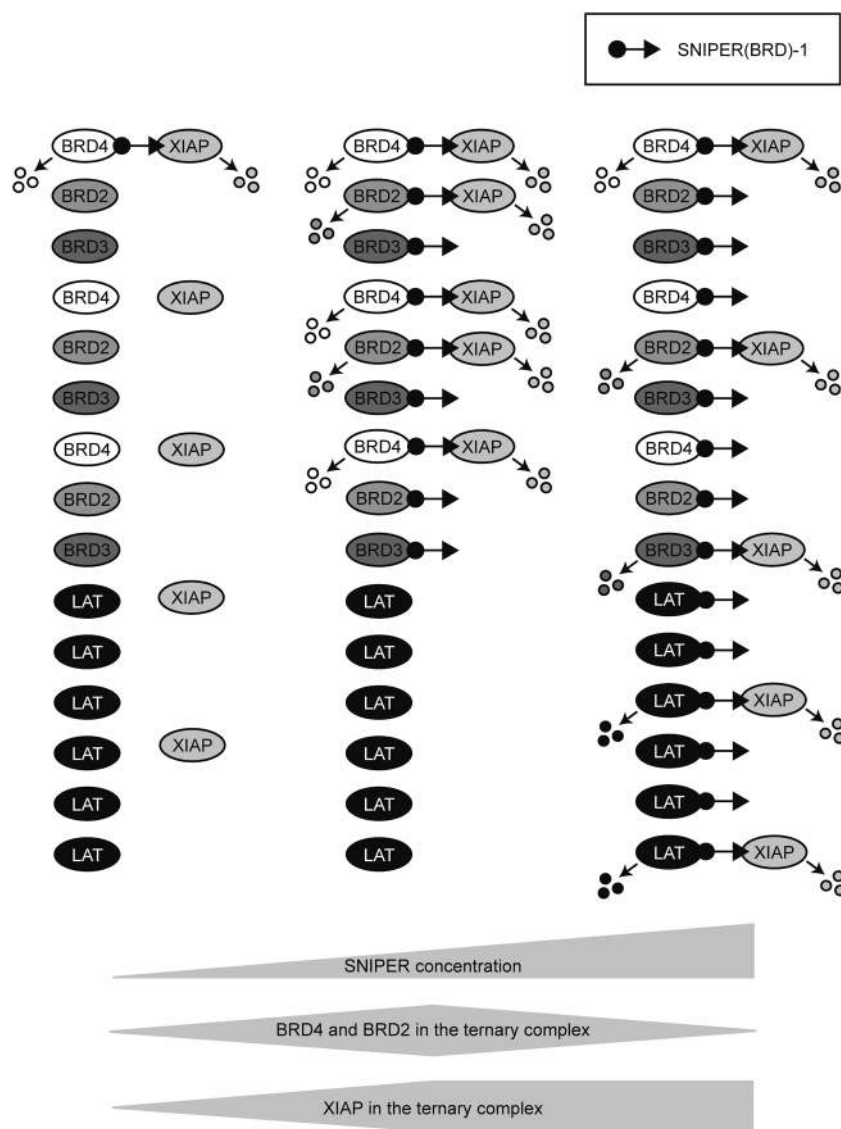


Fig. 7. Schematic Model of the Ternary Complex Formation and Degradation of BRDs and XIAP by SNIPER(BRD)-1

The formation of ternary complexes containing either BRD4 or BRD2 is inhibited at higher concentrations of SNIPER(BRD)-1, accounting for the pharmacological hook effect observed for the degradation of these proteins. However, BRD3 and other low-affinity target proteins also form ternary complexes with SNIPER(BRD)-1, which results in the degradation of XIAP at higher concentrations of SNIPER(BRD)-1. Thus, the pharmacological hook effect was not observed for the degradation of XIAP. LAT: low-affinity target proteins.

we reasoned that SNIPER(BRD)-1 would also induce the degradation of BRD2 and BRD3, resulting in significant levels of XIAP degradation at higher SNIPER concentrations. Figure 6 shows that while the pharmacological hook effect was observed for the degradation of BRD4 and BRD2, it was not clearly observed for the degradation of BRD3. This result suggests that BRD2 forms a ternary complex at low concentrations, as does BRD4, while BRD3 forms the complex at higher concentrations to induce the degradation of XIAP. There are probably additional low-affinity target proteins that can interact with (+)-JQ-1; such proteins could form a ternary complex with SNIPER(BRD)-1 and XIAP to induce the degradation of XIAP at higher concentrations of SNIPER(BRD)-1 (Fig. 7). Thus, the hook effect was observed for BRD4 and BRD2 proteins but not for XIAP.

## Conclusion

In summary, SNIPER(BRD)-1 induces the degradation

of cIAP1 and XIAP along with the intrinsic target protein, BRD4. cIAP1 degradation is triggered by interaction with the IAP antagonist module of SNIPER(BRD)-1 without involving the intrinsic target protein, whereas the degradation of XIAP and BRD4 requires the formation of a ternary complex composed of XIAP, SNIPER(BRD)-1, and BRD4. SNIPER(BRD)-1 also induces the degradation of other target proteins (BRD2 and BRD3) that interact with (+)-JQ-1, allowing the degradation of XIAP at higher concentrations of SNIPER(BRD)-1.

## Experimental

**Chemistry** Chemical synthesis and physicochemical data for SNIPER compounds are provided in the Supplementary Materials.

**Materials** MLN-7243 was purchased from Active Biochem (Maplewood, NJ, U.S.A.). Carbobenzoxy-L-leucyl-L-leucyl-L-leucinal (MG132) was purchased from the Peptide

Institute (Osaka, Japan). (+)-JQ1 was purchased from Sigma-Aldrich (St. Louis, MO, U.S.A.). Biotinylated anti-histidine (His) antibody was from Life Technologies (Carlsbad, CA, U.S.A.). Brij 35 solution was obtained from Merck Millipore (Billerica, MA, U.S.A.). Terbium-labeled streptavidin (Tb-SA) was from Cisbio (Codolet, France). Recombinant His-tagged human XIAP (BIR3, Asn252–Thr356, 895-XB-050) protein was purchased from R&D Systems (Minneapolis, MN, U.S.A.). Recombinant His-tagged human cIAP1 (BIR3, Leu250–Gly350) and cIAP2 (BIR3, Gln238–Ser349) proteins were expressed in *Escherichia coli*, and purified with a Ni-NTA column and gel filtration chromatography. Fluorescein isothiocyanate (FITC)-labeled Smac peptide (FITC-Smac, AVPIAQK(5-FAM)-NH<sub>2</sub>)<sup>41</sup> was synthesized by Scrum (Tokyo, Japan).

**Cell Culture** Human prostate carcinoma LNCaP cells were maintained in RPMI 1640 medium containing 10% fetal bovine serum (FBS) and 100 µg/mL of kanamycin. Cells were treated with various concentrations of SNIPER compounds for the indicated periods.

**Western Blotting** Cells were lysed with sodium dodecyl sulfate (SDS) lysis buffer (0.1M Tris–HCl at pH 8.0, 10% glycerol, 1% SDS) and immediately boiled for 10 min to obtain clear lysates. Protein concentrations were measured using the BCA method (Pierce, Rockford, IL, U.S.A.); equal protein concentrations of each lysate were subjected to SDS-polyacrylamide gel electrophoresis (PAGE) and transferred to polyvinylidene difluoride (PVDF) membranes (Millipore, Darmstadt, Germany) for Western blot analysis using the appropriate antibodies. Immunoreactive proteins were visualized using an Immobilon Western Chemiluminescent HRP Substrate (Merck Millipore) or the Clarity Western ECL Substrate (Bio-Rad, Hercules, CA, U.S.A.); light emission intensity was quantified with a LAS-3000 lumino-image analyzer equipped with Image Gauge v2.3 software (FUJIFILM, Tokyo, Japan). The antibodies used in this study were: anti-BRD4 rabbit monoclonal antibody (mAb) (13440; Cell Signaling Technology, Danvers, MA, U.S.A.), anti-cIAP1 goat polyclonal antibody (pAb) (AF8181; R&D Systems), anti-β-actin mouse mAb (A5316; Sigma-Aldrich), anti-XIAP rabbit pAb (2042; Cell Signaling Technology), anti-BRD2 rabbit mAb (5848; Cell Signaling Technology), and anti-BRD3 mouse mAb (2088C3a; Abcam, Cambridge, U.K.).

**Time-Resolved-Förster Resonance Energy Transfer (TR-FRET) Assay and Data Analysis** TR-FRET assays were carried out using white 384-well flat-bottomed plates (Greiner Bio-One, Frickenhausen, Germany), and the signals were measured with an EnVision plate reader (PerkinElmer, Inc., Waltham, MA, U.S.A.). The solution in each well was excited with a laser ( $\lambda_{\text{ex}} = 337 \text{ nm}$ ) reflected by a dichroic mirror (D400/D505; PerkinElmer, Inc.), and the fluorescence from terbium (Tb) and FITC were detected through two emission filters (CFP 486 for Tb, Emission 515 for FITC; PerkinElmer, Inc.). The assay buffer used in this study comprised 50 mM *N*-2-hydroxyethylpiperazine-*N'*-2-ethanesulfonic acid (HEPES) (pH 7.2–7.5), 10 mM MgCl<sub>2</sub>, 1 mM ethylene glycol bis (2-aminoethyl ether)-*N,N,N',N'*-tetra acetic acid (EGTA), 0.1 mM dithiothreitol (DTT), and 0.01% (v/v) Brij 35. All assays were carried out at room temperature in triplicate or quadruplicate.

The percentage inhibition by the test compounds was calculated according to Eq. 1:

$$\text{Percentage of inhibition} = 100 \times \left( \frac{\mu_{\text{H}} - T}{\mu_{\text{H}} - \mu_{\text{L}}} \right) \quad (1)$$

where  $T$  is the signal from the wells containing the test compounds, and  $\mu_{\text{H}}$  and  $\mu_{\text{L}}$  are the mean signals from the 0 and 100% inhibition control wells, respectively. The IC<sub>50</sub> and the 95% confidence interval of the test compounds were calculated by fitting the data with the four-parameter logistic equation using GraphPad Prism 5 (GraphPad Software, Inc., La Jolla, CA, U.S.A.) or XLfit (IDBS, Guildford, U.K.).

**Measurement of the Inhibitory Activity of IAP–Peptide Interactions** His-IAP proteins (XIAP, cIAP1 or cIAP2), FITC-Smac, Tb-SA, and biotinylated anti-His antibody were mixed in the assay buffer and incubated for more than 1 h at room temperature before being dispensed into the assay plate. Several concentrations of test inhibitors were also dispensed into the plate. All assays were carried out with a final IAP protein concentration of 0.6 nM. The final concentrations of FITC-Smac were as follows: 27 nM for XIAP, 12 nM for cIAP1, and 19 nM for cIAP2. The final concentrations of Tb-SA and the biotinylated anti-His antibody were 0.2 and 0.4 nM, respectively. After 1 h of incubation at room temperature, the TR-FRET signal was measured with an EnVision plate reader. The values for the 0 and 100% controls were those signals obtained in the presence and absence of IAP proteins, respectively.

**Acknowledgments** This work was supported in part by Grants from the Japan Society for the Promotion of Science (KAKENHI Grants 18K06567 to N.O., and 16H05090, 16K15121 and 18H05502 to M.N.), the Japan Agency for Medical Research and Development (AMED Grants JP 17ak0101073 and 18im0210616j0001 to M.N., and JP17cm0106124 and JP18ak0101073 to N.O.), and the Takeda Science Foundation (to N.O.).

**Conflict of Interest** Osamu Ujikawa, Kenichiro Shimokawa, Tomoya Sameshima, Hiroshi Nara, and Nobuo Cho are employees of Takeda Pharmaceutical Co., Ltd.

**Supplementary Materials** The online version of this article contains supplementary materials.

## References

- Ohoka N., Shibata N., Hattori T., Naito M., *Curr. Cancer Drug Targets*, **16**, 136–146 (2016).
- Lai A. C., Crews C. M., *Nat. Rev. Drug Discov.*, **16**, 101–114 (2017).
- Burslem G. M., Crews C. M., *Chem. Rev.*, **117**, 11269–11301 (2017).
- Salami J., Crews C. M., *Science*, **355**, 1163–1167 (2017).
- Okuhira K., Demizu Y., Hattori T., Ohoka N., Shibata N., Nishimaki-Mogami T., Okuda H., Kurihara M., Naito M., *Cancer Sci.*, **104**, 1492–1498 (2013).
- Shibata N., Miyamoto N., Nagai K., Shimokawa K., Sameshima T., Ohoka N., Hattori T., Imaeda Y., Nara H., Cho N., Naito M., *Cancer Sci.*, **108**, 1657–1666 (2017).
- Shimokawa K., Shibata N., Sameshima T., Miyamoto N., Ujikawa O., Nara H., Ohoka N., Hattori T., Cho N., Naito M., *ACS Medicinal Chemistry Letters*, **8**, 1042–1047 (2017).
- Ohoka N., Nagai K., Shibata N., Hattori T., Nara H., Cho N., Naito M., *Cancer Sci.*, **108**, 1032–1041 (2017).
- Ohoka N., Nagai K., Hattori T., Okuhira K., Shibata N., Cho N., Naito M., *Cell Death Dis.*, **5**, e1513 (2014).

- 10) Ohoka N., Misawa T., Kurihara M., Demizu Y., Naito M., *Bioorg. Med. Chem. Lett.*, **27**, 4985–4988 (2017).
- 11) Ohoka N., Okuhira K., Ito M., Nagai K., Shibata N., Hattori T., Ujikawa O., Shimokawa K., Sano O., Koyama R., Fujita H., Teratani M., Matsumoto H., Imaeda Y., Nara H., Cho N., Naito M., *J. Biol. Chem.*, **292**, 4556–4570 (2017).
- 12) Lai A. C., Toure M., Hellerschmied D., Salami J., Jaime-Figueroa S., Ko E., Hines J., Crews C. M., *Angew. Chem.*, **55**, 807–810 (2016).
- 13) Remillard D., Buckley D. L., Paulk J., Brien G. L., Sonnett M., Seo H. S., Dastjerdi S., Wuhr M., Dhe-Paganon S., Armstrong S. A., Bradner J. E., *Angew. Chem.*, **56**, 5738–5743 (2017).
- 14) Zhou B., Hu J., Xu F., Chen Z., Bai L., Fernandez-Salas E., Lin M., Liu L., Yang C. Y., Zhao Y., McEachern D., Przybranowski S., Wen B., Sun D., Wang S., *J. Med. Chem.*, **61**, 462–481 (2018).
- 15) Shibata N., Nagai K., Morita Y., Ujikawa O., Ohoka N., Hattori T., Koyama R., Sano O., Imaeda Y., Nara H., Cho N., Naito M., *J. Med. Chem.*, **61**, 543–575 (2018).
- 16) Winter G. E., Buckley D. L., Paulk J., Roberts J. M., Souza A., Dhe-Paganon S., Bradner J. E., *Science*, **348**, 1376–1381 (2015).
- 17) Bondeson D. P., Mares A., Smith I. E., Ko E., Campos S., Miah A. H., Mulholland K. E., Routly N., Buckley D. L., Gustafson J. L., Zinn N., Grandi P., Shimamura S., Bergamini G., Faelth-Savitski M., Bantscheff M., Cox C., Gordon D. A., Willard R. R., Flanagan J. J., Casillas L. N., Votta B. J., den Besten W., Famm K., Kruidenier L., Carter P. S., Harling J. D., Churcher I., Crews C. M., *Nat. Chem. Biol.*, **11**, 611–617 (2015).
- 18) Raina K., Lu J., Qian Y., Altieri M., Gordon D., Rossi A. M., Wang J., Chen X., Dong H., Siu K., Winkler J. D., Crew A. P., Crews C. M., Coleman K. G., *Proc. Natl. Acad. Sci. U.S.A.*, **113**, 7124–7129 (2016).
- 19) Ohoka N., Morita Y., Nagai K., Shimokawa K., Ujikawa O., Fujimori I., Ito M., Hayase Y., Okuhira K., Shibata N., Hattori T., Sameshima T., Sano O., Koyama R., Imaeda Y., Nara H., Cho N., Naito M., *J. Biol. Chem.*, **293**, 6776–6790 (2018).
- 20) Fulda S., Vucic D., *Nat. Rev. Drug Discov.*, **11**, 109–124 (2012).
- 21) Deveraux Q. L., Reed J. C., *Genes Dev.*, **13**, 239–252 (1999).
- 22) Salvesen G. S., Duckett C. S., *Nat. Rev. Mol. Cell Biol.*, **3**, 401–410 (2002).
- 23) Deveraux Q. L., Takahashi R., Salvesen G. S., Reed J. C., *Nature (London)*, **388**, 300–304 (1997).
- 24) Hao Y., Sekine K., Kawabata A., Nakamura H., Ishioka T., Ohata H., Katayama R., Hashimoto C., Zhang X., Noda T., Tsuruo T., Naito M., *Nat. Cell Biol.*, **6**, 849–860 (2004).
- 25) Suzuki Y., Nakabayashi Y., Takahashi R., *Proc. Natl. Acad. Sci. U.S.A.*, **98**, 8662–8667 (2001).
- 26) Kikuchi R., Ohata H., Ohoka N., Kawabata A., Naito M., *J. Biol. Chem.*, **289**, 3457–3467 (2014).
- 27) Imoto I., Tsuda H., Hirasawa A., Miura M., Sakamoto M., Hirohashi S., Inazawa J., *Cancer Res.*, **62**, 4860–4866 (2002).
- 28) Imoto I., Yang Z. Q., Pimkhaokham A., Tsuda H., Shimada Y., Imamura M., Ohki M., Inazawa J., *Cancer Res.*, **61**, 6629–6634 (2001).
- 29) Tamm I., Kornblau S. M., Segall H., Krajewski S., Welsh K., Kitada S., Scudiero D. A., Tudor G., Qui Y. H., Monks A., Andreeff M., Reed J. C., *Clin. Cancer Res.*, **6**, 1796–1803 (2000).
- 30) Jaffer S., Orta L., Sunkara S., Sabo E., Burstein D. E., *Hum. Pathol.*, **38**, 864–870 (2007).
- 31) Wang J., Liu Y., Ji R., Gu Q., Zhao X., Liu Y., Sun B., *Hum. Pathol.*, **41**, 1186–1195 (2010).
- 32) Foster F. M., Owens T. W., Tanianis-Hughes J., Clarke R. B., Brennan K., Bundred N. J., Streuli C. H., *Breast Cancer Research: BCR*, **11**, R41 (2009).
- 33) Yang L., Cao Z., Yan H., Wood W. C., *Cancer Res.*, **63**, 6815–6824 (2003).
- 34) Cohen P., Tcherpakov M., *Cell*, **143**, 686–693 (2010).
- 35) Wang S., Bai L., Lu J., Liu L., Yang C. Y., Sun H., *J. Mammary Gland Biol. Neoplasia*, **17**, 217–228 (2012).
- 36) Varfolomeev E., Blankenship J. W., Wayson S. M., Fedorova A. V., Kayagaki N., Garg P., Zobel K., Dynek J. N., Elliott L. O., Wallweber H. J., Flygare J. A., Fairbrother W. J., Deshayes K., Dixit V. M., Vucic D., *Cell*, **131**, 669–681 (2007).
- 37) Vince J. E., Wong W. W., Khan N., Feltham R., Chau D., Ahmed A. U., Benetatos C. A., Chunduru S. K., Condon S. M., McKinlay M., Brink R., Leverkus M., Tergaonkar V., Schneider P., Callus B. A., Koentgen F., Vaux D. L., Silke J., *Cell*, **131**, 682–693 (2007).
- 38) Bertrand M. J., Milutinovic S., Dickson K. M., Ho W. C., Boudreault A., Durkin J., Gillard J. W., Jaquith J. B., Morris S. J., Barker P. A., *Mol. Cell*, **30**, 689–700 (2008).
- 39) Sekine K., Takubo K., Kikuchi R., Nishimoto M., Kitagawa M., Abe F., Nishikawa K., Tsuruo T., Naito M., *J. Biol. Chem.*, **283**, 8961–8968 (2008).
- 40) Filippakopoulos P., Qi J., Picaud S., Shen Y., Smith W. B., Fedorov O., Morse E. M., Keates T., Hickman T. T., Felletar I., Philpott M., Munro S., McKeown M. R., Wang Y., Christie A. L., West N., Cameron M. J., Schwartz B., Heightman T. D., La Thangue N., French C. A., Wiest O., Kung A. L., Knapp S., Bradner J. E., *Nature (London)*, **468**, 1067–1073 (2010).
- 41) Nikolovska-Coleska Z., Wang R., Fang X., Pan H., Tomita Y., Li P., Roller P. P., Krajewski K., Saito N. G., Stuckey J. A., Wang S., *Anal. Biochem.*, **332**, 261–273 (2004).